Progress In Electromagnetics Research C, Vol. 110, 181–195, 2021

Tunable Triple Band-Notched UWB Antenna Using Single EBG and Varactor Diode

Vijay R. Kapure[1, *], Pramod P. Bhavarthe[2], and Surendra S. Rathod[3]

Abstract—In this paper, a UWB monopole antenna with triple band-notch characteristics using single TBMV-EBG (Triple band multi-via electromagnetic bandgap) unit cell is proposed and demonstrated. The antenna with a fork-type radiating patch with TBMV-EBG is simulated using Ansys HFSS. Measurement results show triple band-notches at 3.39, 5.78, and 8.60 GHz, respectively, which are in good agreement with simulation results. The proposed antenna has bi-directional pattern in E-plane and omnidirectional pattern in H-plane. Moreover, tunable characteristics of the proposed antenna using a single varactor diode are also presented. By changing the capacitance of varactor, the band-notched antenna is effectively tuned from 2.69–3.46, 5.71–7.84, and 8.40–8.50 GHz. The same antenna structure can be operated at different band notching modes depending upon the varactor's capacitance. Therefore, the proposed UWB antenna will prove to be a promising candidate wherein multi-band rejections using single TBMV-EBG unit cell and tunability using one varactor diode are desirable.

1. INTRODUCTION

Ultra-wideband (UWB) systems have become important for short range, high data rate, low power consumption, and indoor data communication. In 2002, Federal Communications Commission(FCC) allocated the frequency band of 3.1 to 10.6 GHz for UWB systems. In this allocated UWB, other narrowband systems like wireless local area network (WLAN) for IEEE 802.11a operating at (5.15–5.35) and (5.725–5.825) GHz & WIMAX (3.3–3.6) GHz and X-band (8–12) GHz are already present. Therefore, in order to avoid electromagnetic interference, UWB antenna should reject these types of narrowband systems. In recent years, many techniques have been proposed to reject these narrow bands. In [1–4], narrow band notches are achieved by etching slots on radiating elements. In [5, 6], quad and quintuple UWB band-notched antennas are reported using CSRRs and RCSRRs, respectively. However, this technique of inferring the antenna to get multi-bands affects the performance of antenna. To overcome this problem, placing a parasitic element near the feed line of antenna is proposed in [7–16]. In [7], a hexagon-shaped monopole UWB antenna with two same size edge located via (ELV) EBG cells are placed near the feed line to get dual band notches at 3.5 GHz and 5.5 GHz. In [8], a UWB circular monopole antenna with dual band notch rejection is achieved using four center located via (CLV) EBGs. In [9], two modified mushroom type semicircular EBG structures with dissimilar sizes are placed near the feed line to produce dual band notch rejection in WIMAX band. In [10], to get triple band notch characteristics, three EBG unit cells are used. In [11], a UWB monopole antenna with two spiral EBGs, one on front side near the feed and the other on back side, is used to produce dual band notches at the upper and lower WLAN frequencies. In [12], an antenna is reported with

Received 22 January 2021, Accepted 23 February 2021, Scheduled 27 February 2021

* Corresponding author: Vijay Ramesh Kapure (vijaykapure777@gmail.com).

[1] Department of Electronics Engineering, Sardar Patel Institute of Technology, Andheri (West), Mumbai-400058, India. [2] Department of Electronics and Telecommunication Engineering, Padmabhushan Vasantdada Patil Pratishthan's College of Engineering, Sion, Mumbai-400022, India. [3] Department of Electronics Engineering, Sardar Patel Institute of Technology, Andheri (West), Mumbai-400058, India.

dual band notches by placing two ELV MT-EBGs near the feed line of elliptical monopole antenna. In [13], a single band notch at 5.5 GHz is obtained by using four conventional MT-EBGs. [14] reports a UWB band-notched antenna producing single notch at 3.5 GHz using two EBGs around the feed line. In [15], =single EBG is used to get dual band notches at 4.51 GHz and 5.89 GHz. Also, in [16] triple band notches are obtained by placing two different EBGs near the feed line of the antenna. Due to space restriction and coupling between multi-parasitic elements, it is difficult to achieve multi-notch characteristics for a UWB monopole antenna with minimum cells. The works presented in [7–16] have failed to design multi-notches, i.e., triple notch characteristics for UWB monopole antenna with single EBG cell. In Section 2, we give the application of TBMV EBG to overcome the above problem. The proposed UWB antenna behaves as triple band notches using single unit cell of TBMV-EBG. Also the tuning characteristics of triple band-notched antenna using varactor diode are discussed in Section 3.

2. ANTENNA DESIGN PARAMETERS AND SIMULATION RESULTS

A reference fork-type monopole antenna [9] is shown in Fig. 1 with $\epsilon_r = 2.2$, $\tan\delta = 0.0009$. The antenna is etched with a size of $35 \times 35\,\text{mm}^2$ on a substrate with height $h = 0.8\,\text{mm}$. The ground plane of the reference antenna is etched by a quasi semi-circular slot. The width of microstrip feed is kept as 1.5 mm, and the other parameters of proposed antenna are: $(L_1) = 35\,\text{mm}$, $(W_1) = 35\,\text{mm}$, $(L_2) = 12\,\text{mm}$, $(L_3) = 13.6\,\text{mm}$, $(L_4) = 2.1\,\text{mm}$, $(L_5) = 9\,\text{mm}$, $(L_6) = 1.6\,\text{mm}$, $(W_2) = 6\,\text{mm}$, $(W_3) = (W_4) = 2.1\,\text{mm}$, $(W_5) = 1.8\,\text{mm}$. This fork type of monopole antenna is used as reference antenna for further design.

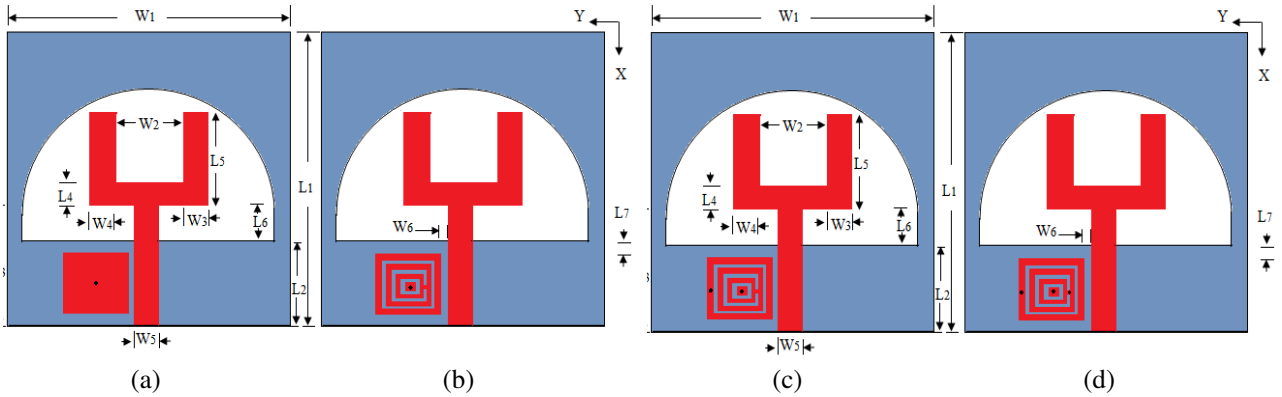

Figure 1. UWB antenna configurations, (a) Antenna-I with MT-CLV EBG, (b) Antenna-II with intermediate EBG (one via), (c) Antenna-III with intermediate EBG (two vias) and (d) Antenna-IV with proposed TBMV-EBG (three vias).

2.1. Ultra-Wideband Antenna Configurations and Analysis

Fork-type UWB antennas with different evolution stages of EBG configuration are shown in Fig. 1. Fig. 1(a) shows Antenna-I configuration with conventional mushroom-type center located via an electromagnetic bandgap structure (MT-CLV EBG). Fig. 1(b) shows Antenna-II configuration with a modified EBG having outer ring, middle ring, inner ring and a via placed at a center located square patch. Antenna-III configuration in Fig. 1(c) depicts an intermediate stage of EBG with the addition of one more via at the outer ring. Finally, Antenna-IV configuration with TBMV-EBG (triple band multi-via electromagnetic bandgap structure) is shown in Fig. 1(d). This TBMV-EBG unit cell consists of three vias at the outer ring, center located square patch, and on the joint between middle and inner rings, respectively. The TBMV-EBG unit cell design parameters along with parametric analysis are explained in this section.

All the antenna configurations discussed earlier are simulated, and voltage standing wave ratio (VSWR) is plotted as shown in Fig. 2. Antenna-I with MT-CLV EBG shows a single notch at 7.23 GHz. When the configuration of Antenna-II is simulated, dual closely spaced notches at 7.87 GHz and 8.47 GHz

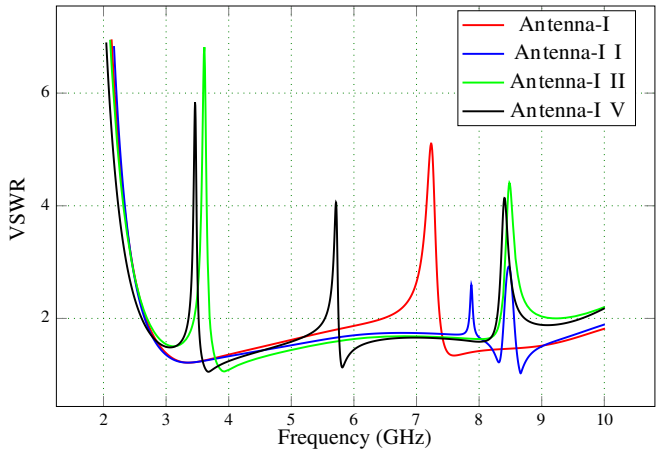

Figure 2. Simulated VSWR of different antenna configurations from Antenna-I to Antenna-IV with TBMV-EBG.

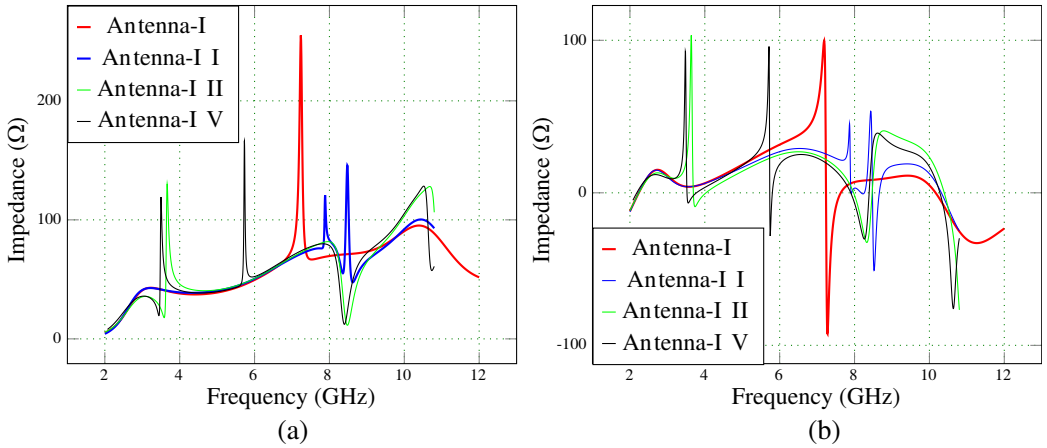

Figure 3. Simulated impedance of different antenna configurations, (a) Real part, and (b) Imaginary part.

are obtained. Antenna-III also behaves as a dual-band notched antenna producing sharp notches at 3.61 GHz and 8.48 GHz, respectively. When Antenna-IV with TBMV-EBG is simulated, triple-band notched characteristics are observed at 3.46 GHz, 5.71 GHz, and 8.40 GHz, respectively. In order to verify the band-notch characteristics of all configurations of antennas shown in Fig. 1, simulations with respect to impedance are also carried out. Fig. 3 shows real and imaginary parts of impedance for all antenna configurations. From Fig. 3(a), it is observed that the real part of impedance goes away from 50 Ω for all configurations of antennas at the notched frequencies due to impedance mis-matching. Similarly, imaginary part of impedance also goes away from 0 Ω at the specific notch frequencies which can be seen from Fig. 3(b).

2.2. Proposed UWB Antenna with TBMV EBG

EBG generally referred as metamaterials does exhibit specific properties. The surface impedance of EBG structure is similar to that of a parallel resonant LC circuit which can be modelled using effective surface impedance model. The surface impedance (Z_s) and resonance frequency (f_c) are given as [17, 18]

$$Z_s = \frac{j\omega L}{1 - \omega^2 LC} \tag{1}$$

and

$$f_c = \frac{1}{2\pi\sqrt{LC}} \tag{2}$$

where the inductance (L) and capacitance (C) are calculated as

$$L = \mu_0 h \tag{3}$$

and

$$C = \frac{x_1\epsilon_o(\epsilon_r + 1)}{\pi} \cosh^{-1}\left\{\frac{2x_1 + k}{k}\right\} \tag{4}$$

where (μ_0) = permeability of free space, (h) = substrate height, (x_1) = width of each EBG cell, (k) = gap between two EBG cell, (ϵ_r) = dielectric constant of the substrate, and (ϵ_0) = permittivity of free space. To design a TBMV EBG structure, three series LC resonant circuit per unit cell are required. To achieve this, three vias with different slots are introduced in the proposed EBG as shown in Fig. 4. The proposed TBMV-EBG cell is with one outer ring, inner ring, and C-type of slot between inner and outer rings [32].

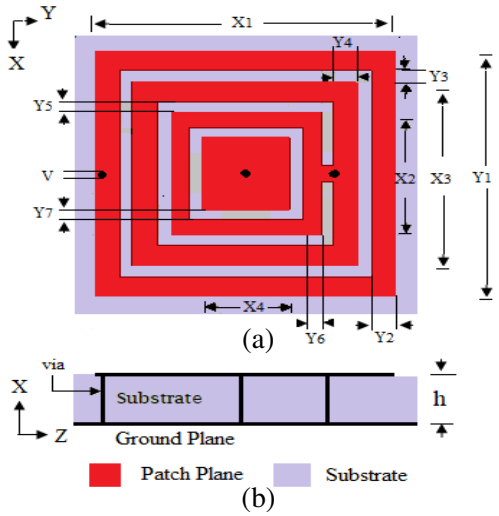

Figure 4. TBMV-EBG unit cell, (a) top view, (b) side view.

The UWB fork-type antenna with a single TBMV EBG cell is shown in Fig. 1(d). Simulated voltage standing wave ratio (VSWR) of the fork-type reference antenna is shown in Fig. 5. A good impedance match is obtained for UWB range (3.1–10.6) GHz with VSWR < 2 without any band notches. The EBG cell is placed near the feed line of UWB monopole antenna and simulated using Ansys HFSS. Parameters of the reference antenna are same as mentioned earlier in this section. Optimized parameters of TBMV EBG cell are: diameter of each via (v) = 0.2 mm, substrate dielectric constant (ϵ_r) = 2.2, substrate height (h) = 0.8 mm, width of outer ring (y_2) = 1 mm, width of outer ring slot (y_3) = 0.4 mm, width of middle ring (y_4) = 0.7 mm, width of C-type slot (y_5) = 0.3 mm, width of inner ring (y_6) = 0.5 mm, width of inner ring slot (y_7) = 0.2 mm, (x_2) = 3.2 mm, (x_3) = 5.2 mm, width of center located square patch (x_4) = 1.8 mm, square patch width (x_1) = 8 mm, width of joint between middle and inner ring (j) = 0.3 mm. The gap between the feed line and EBG cell is kept as (W_6) = 0.2 mm, and the distance between EBG cell and upper edge of quasi semi-circular slot is (L_7) = 1.2 mm. Simulated VSWRs of UWB monopole antenna with and without TBMV EBG are shown in Fig. 5. It is observed that there is no band notch for UWB monopole antenna without TBMV EBG, whereas with TBMV EBG cell, UWB antenna produces triple band notch frequencies observed at 3.46 GHz, 5.71 GHz, and 8.40 GHz (VSWR > 2 GHz) which proves that TBMV EBG exhibits triple band notch characteristics. The first, second, and third notches are obtained from 3.34 GHz to 3.58 GHz, 5.44 GHz to 5.96 GHz, and 8.31 GHz to 8.50 GHz with notch bandwidths of 0.24 GHz, 0.52 GHz, and 0.19 GHz, respectively. Measured VSWR

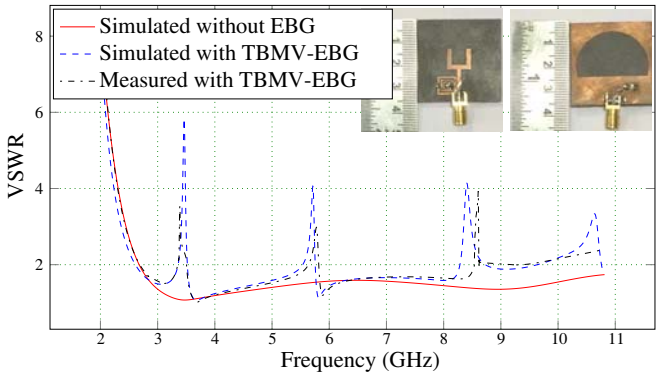

Figure 5. Fabricated Prototype, simulated and measured VSWR of fork-type monopole antenna with and without TBMV-EBG.

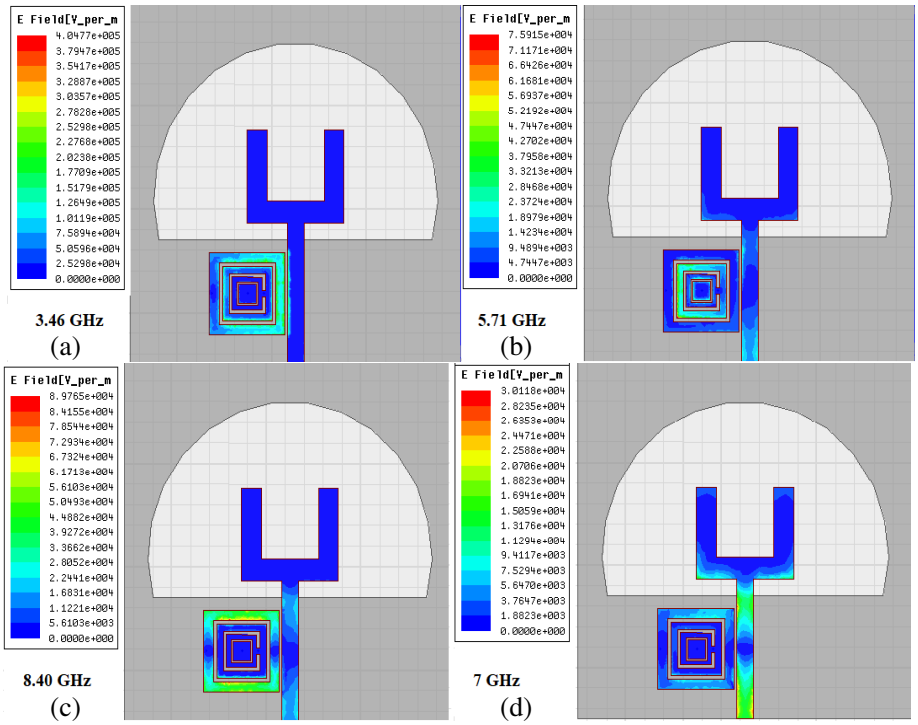

Figure 6. Surface current distributions of UWB band-notched antenna with TBMV-EBG at (a) 3.46 GHz, (b) 5.71 GHz, (c) 8.40 GHz, and (d) 7 GHz.

of UWB fork-type antenna with TBMV-EBG is plotted in Fig. 5. From the graph it is observed that the simulated and measured results are in good agreement.

Surface current distributions at 3.46 GHz, 5.71 GHz, 8.40 GHz, and 7 GHz for the first, second, third notches and operating frequency of UWB antenna are shown in Fig. 6, respectively. From Fig. 6(a), it is observed that at 3.46 GHz the surface current is mostly concentrated on the outer ring of TBMV-EBG which is close to the feed line. The surface current distribution at 5.71 GHz is shown in Fig. 6(b). The notch obtained at this frequency is mainly due to the inner ring of EBG. Since the inner ring is far away from feed line, reduction in VSWR is observed. Fig. 6(c) shows the even surface current distribution on the opposite arms of outer ring of TBMV-EBG producing third notch at 8.40 GHz. Fig. 6(d) shows the surface current distribution at the operating frequency, i.e., 7 GHz. The current is more along the feed line and lower edge of fork-type patch with almost negligible effect on EBG.

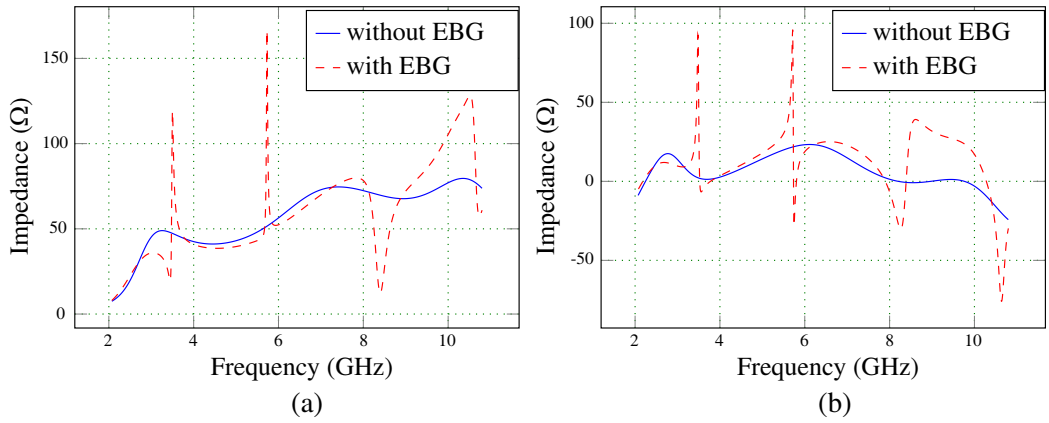

Figure 7. Simulated impedance of fork type monopole antenna without TBMV-EBG and with TBMV-EBG, (a) real part, and (b) imaginary part.

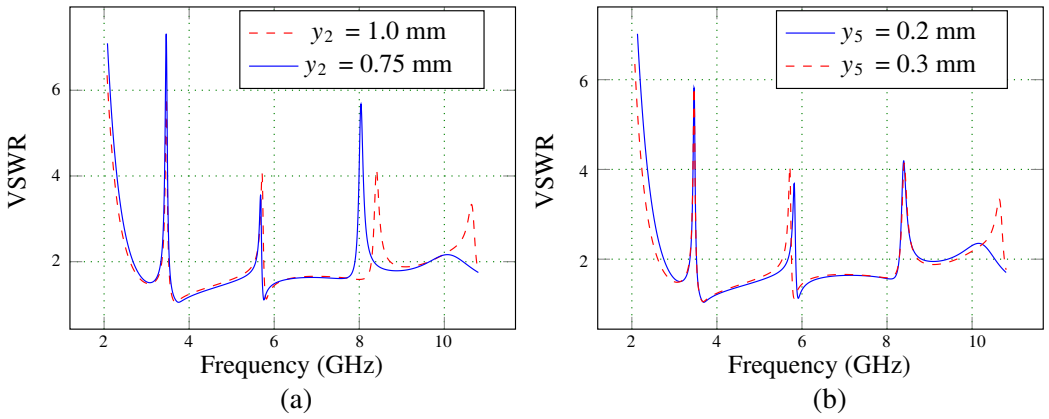

Figure 8. (a) Effect of the outer ring on the center frequency of the band-notch, and (b) effect of the gap between middle ring and inner ring on the center frequency of the band-notch.

Simulated real and imaginary parts of impedances of reference antenna with and without TBMV EBG are shown in Fig. 7(a) and (b), respectively. Real and imaginary parts of the impedance go away from 50 Ω and 0 Ω line, respectively for all notch frequencies. The effects of parameters of TBMV EBG on the notch band center frequency are shown in Fig. 8 and Fig. 9(a). Fig. 8(a) shows the effect of the width of outer ring on the center frequency of the band-notch of antenna. By varying the outer ring width (y_2), a noticeable change in the third notch frequency is observed without any change in the first and second notches. Fig. 8(b) shows effect of the gap between middle ring and inner ring (y_5) on the center frequency of the band-notch. Variation in (y_5) produces changes in second notch frequency only with negligible effect on the first and third notches. The effect of the gap between outer ring and middle ring (y_3) on the center frequency of the band-notch is shown in Fig. 9(a). Changing (y_3) shows observable change in the first notch frequency without any significant changes in remaining two notch frequencies. Measured and simulated gains of antenna with TBMV EBG are shown in Fig. 9(b). Significant drop in gain is observed at the triple band notch frequencies with a good performance for other frequencies.

Simulations of the proposed UWB antenna with TBMV-EBG are also conducted using FR4 epoxy ($\tan\delta = 0.02$, $\epsilon_r = 4.4$) and air ($\epsilon_r = 1$) compared with Rogers substrate ($\tan\delta = 0.0009$, $\epsilon_r = 2.2$). Simulated VSWRs for different substrates are shown in Fig. 10. It is observed from the graph that with Rogers as substrate, triple band notches are produced for UWB applications specified by FCC (3.1–10.6) GHz. Radiation patterns of reference antenna with TBMV EBG in E-plane and H-plane at

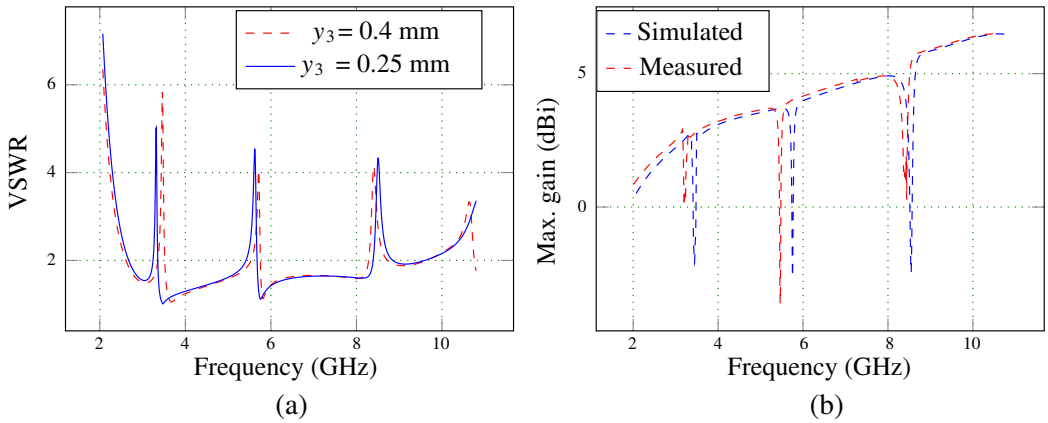

Figure 9. (a) Effect of the gap between outer ring and middle ring on the center frequency of the band-notch, and (b) antenna gain.

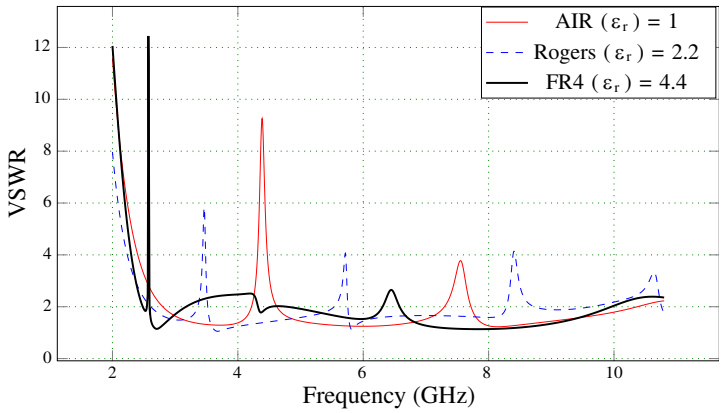

Figure 10. Simulated VSWR of fork-type antenna with TBMV-EBG for different substrates.

4.00 GHz, 5.71 GHz, 6.00 GHz, and 8.00 GHz are shown in Fig. 11. Since the UWB antenna is band-notched at 5.71 GHz, the radiation characteristics are distorted whereas the antenna has bi-directional pattern in E-plane and omnidirectional pattern in H-plane for other frequencies. It can also be observed from Fig. 11 that as the frequency increases, the antenna does not obey perfect E-plane and H-plane radiation characteristics.

2.3. Fabrication and Measurement

Fork type of UWB antenna with single cell of TBMV EBG is printed on a Rogers Diclad 880 substrate with dielectric constant $(\epsilon_r) = 2.2$, $h = 0.8$ mm, and $\tan\delta = 0.0009$ as shown in Fig. 5. The measurements are conducted with an Agilent N9926A network analyzer with the highest measurable frequency 14.00 GHz. A 50 Ω SMA connector is connected at the end of the feed line. The measured VSWR of fabricated fork-type antenna with TBMV EBG is shown in Fig. 5. From the results, it is observed that three band notches are obtained with a slight difference between simulation and measurement results. These differences are mainly due to the reasons mentioned in [12]. In the measurements, we obtain band-notch center frequencies with 3.39 GHz, 5.78 GHz, and 8.60 GHz (VSWR > 2 GHz). From the simulation and measurement results it is proved that using single cell of TBMV EBG at the feed line of UWB monopole antenna, triple band notches can be achieved. Comparison of different EBGs and proposed TBMV EBG structure used for getting multiple band notches in UWB monopole antenna at the fed line is given in Table 1.

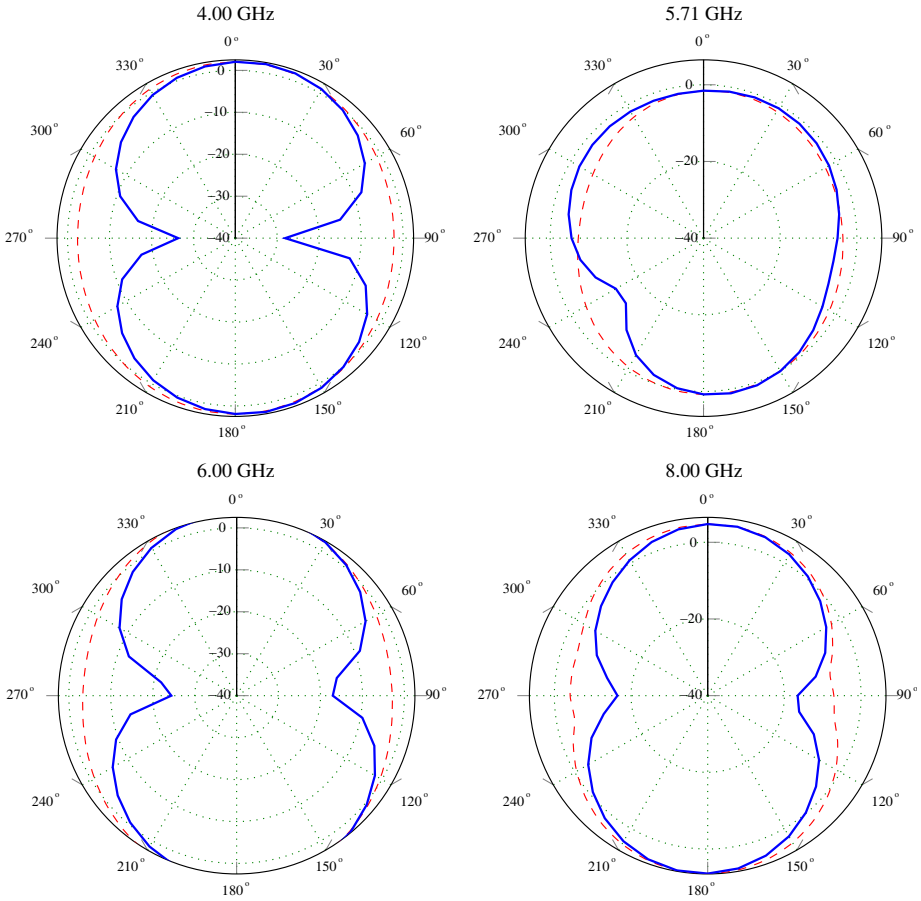

Figure 11. Radiation pattern for E-plane (x-z), and H-plane (y-z) of fork-type monopole antenna with TBMV-EBG (— E-plane, and --- H-plane).

Table 1. Comparison of TBMV-EBG and other EBG structures used for getting band-notch in UWB monopole antenna at fed line.

Ref.	ϵ_r/h (mm)	No. of EBG	No. of Notches	Notched center frequencies (GHz)
[7]	4.5/1.59	02	Dual	3.5/5.5/N.A
[8]	4.4/1.60	04	Dual	3.44/5.44/N.A
[9]	2.65/1.00	02	Dual	5.2/5.8/N.A
[10]	3.38/0.8	03	Triple	3.27/5.27/5.71
[11]	3.66/0.762	02	Dual	5.2/5.8/N.A
[12]	4.5/1.00	02	Dual	5.31/5.80/N.A
[13]	3.8/0.8	04	Single	5.5/N.A/N.A
[14]	4.4/1.60	02	Single	3.5/N.A/N.A
[15]	4.4/1.00	01	Dual	4.54/5.92/N.A
[16]	4.4/1.60	02	Triple	3.65/5.45/7.5
P. W.	**2.2/0.8**	**01**	**Triple**	**3.39/5.78/8.60**

P. W. = Proposed work., N.A = Not applicable

3. TUNABLE UWB ANTENNA WITH TBMV-EBG AND VARACTOR DIODE

Over a decade, band-notched antennas with tuning capability have certainly gained tremendous significance. However, it is known that as frequency in some bands varies from one region to another, antennas once designed and fabricated for fixed notch-frequencies becomes fruitless for other applications. In order to make the effective use of designed band-notched antennas for other frequencies, continuously tuning characteristics need to be incorporated. Embedding active devices such as switch, MEMS, P-I-N diodes in band-notched antenna design, switching functionality is achieved. Antennas designed with these active devices can be switched possibly only between two frequencies based on their ON and OFF status. So, to achieve fine tunability, band-notched antenna designs with varactor diode as an active device are mostly preferred. By changing the capacitance of varactor diode operated under different reverse bias, band-notched antennas can be effectively tuned for specific desired frequency of interest along the spectrum.

Various techniques are employed in band-notched antennas to produce notches at specific frequency of interest. However, these band notches are achieved by etching slots on radiating elements, using resonators or with multi-parasitic elements around the feed line [7–16, 19–31]. In order to achieve multiple band-notches, UWB antennas should not only make effective use of the space around the radiating patch but also be able to minimize coupling effects with less parasitic elements near the feed line. The work presented in this manuscript overcomes this issue by placing a single unit cell of TBMV-EBG near the feed line of UWB monopole antenna. Moreover, frequency reconfiguration of the proposed triple band-notched antenna is obtained by using single varactor diode in the EBG design. The notched bands are effectively tuned by changing the capacitance of varactor diode. The varactor SMP1231-079LF from Skyworks is used for the design. The configuration of fork-type antenna with varactor loaded TBMV-EBG and the spice model of varactor are shown in Fig. 12(a) and (b), respectively. Previously, various reconfigurable band-notched antennas using more active devices such as capacitors and varactors have been reported in [19–31]. In [19], open loop resonators (OLRs) are used around the feed line of antenna to produce single band-notch, and the antenna is tuned from 5.1 to 5.9 GHz using two varactors embedded in the OLRs. Reconfiguration with two pin-diodes and two varactor diodes inside meander line stubs are reported in [20]. Depending upon the on/off status of pin diodes in combination with varactors, single notched band is tuned from 4.2 to 4.8 GHz and 5.8- to 6.5 GHz, respectively. In [21], UWB antenna is band-notched using inverted T-slot and U-shaped slots and tuned independently with two varactor diodes from 3.5 to 4.3 GHz and 5.3 to 6.05 GHz. The antenna in [22] is etched on the feed line to produce single notch which is tuned from 4.3 to 6.1 GHz. [23] reports a tunable band notched UWB heart-shaped planar monopole antenna with a annular slot producing single notch. By varying capacitance of the varactor, the notch is tuned from 4.62 to 5.83 GHz. In [24], resonators are used to produce dual notches at WIMAX and WLAN, respectively. Inserting two capacitors within the resonators, the antenna tunes only the WIMAX band notch from 3.0 to 4.0 GHz with fixed WLAN notch frequency. In [25], a similar dual band notch antenna is reported and tuned to produce dual band notches using four capacitors within the resonators. In [26], tuning of single band from 5.8 to 6.9 GHz is achieved using two varactor diodes. In [27], a CSRR etched triple band notched antenna is tuned using three varactor diodes. In [28, 29], capacitors are embedded within the resonators to tune WLAN band from 5.0 to 6.0 GHz. In [30], triple band notching and tuning are achieved with open ended stubs and three varactors, respectively. In [31], two EBG structures, namely TVEL and fractal, are used to produce dual band notches at WIMAX and WLAN bands, respectively. The EBG structures are loaded with two varactor diodes and tuned independently between 2.8–4.0 GHz and 4.7–6.2 GHz. The works reported in [19–21, 24–31] have either managed to produce tunability with more varactors/capacitors or are able to tune only single notch-band [22, 23]. Considering the power supply constraints and biasing circuit's complexity, it is always desirable to design multi-band notch antennas with minimum active devices for continuous tuning.

In our previous work [32], switching characteristics of band-notched antenna using single P-I-N diode are demonstrated. In this work in order to achieve fine tunability, the proposed triple band-notched UWB antenna is made tunable by incorporating one active device, i.e., varactor diode within single EBG unit cell. The varactor diode is inserted between outer and middle rings of TBMV-EBG as shown in Fig. 12 and is operated under reverse bias voltage for different values of capacitances. The state of art reported in Table 2 shows the comparison of various band-notched antennas with the

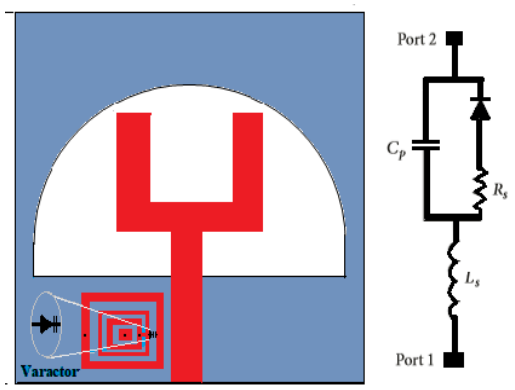

Figure 12. (a) UWB antenna with TBMV-EBG and Varactor diode, (b) spice model of Varactor.

Table 2. Comparison of TBMV-EBG and other EBG structures used for getting band-notches and reconfiguration in UWB antennas.

Ref.	Band-Notch Technique Used	Reconfig. Done With	Active Devices Used	Tuning Frequencies (GHz)
[19]	OLR	Varactor	02	5.1–5.9
[20]	Stub	P-I-N/Varactor	04	4.2–4.8/5.8–6.5
[21]	Slot	Varactor	02	3.5–4.3/5.3–6.05
[22]	Slot	Varactor	01	4.3–6.1
[23]	Slot	Varactor	01	4.62–5.83
[24]	Resonator	Capacitor	02	3.0–4.0
[25]	Resonator	Capacitor	04	2.9–3.1/5.8–7.0
[26]	Resonator	Varactor	02	5.8–6.9
[27]	CSRR slots	Varactor	03	1.5–2.1/2.2–2.6/3.0–3.7
[28]	Resonator	Capacitor	02	5.0–6.0
[29]	Resonator	Capacitor	02	5.0–6.0
[30]	Open Stubs	Varactor	03	3.3–3.5/5.2–5.4/5.7–5.9
[31]	EBG	Varactor	02	2.8–4.0/4.7–6.2
P. W.	**EBG**	**Varactor**	**01**	**2.6–3.4/5.7–7.8/8.4–8.5**

OLR = Open Loop Resonator, EBG = Electromagnetic Bandgap Structure,
CSRR = Complementary split-ring resonators, P. W. = Proposed work.

proposed antenna in terms of tunability. From the comparison, it is observed that the proposed antenna will prove to be the promising candidate wherein tuning with multi-bands using a single active device is desirable.

4. RESULTS AND DISCUSSIONS

Experimental setup and fabricated prototype of tunable band-notched UWB antenna with varactor loaded TBMV-EBG are shown in Fig. 13 and Fig. 14, respectively. The fork type UWB antenna design parameters and TBMV-EBG unit cell dimensions are kept same as discussed in earlier sections. Rogers material with loss tangent $\tan\delta = 0.0009$ and permittivity $\epsilon_r = 2.2$ is used as substrate for

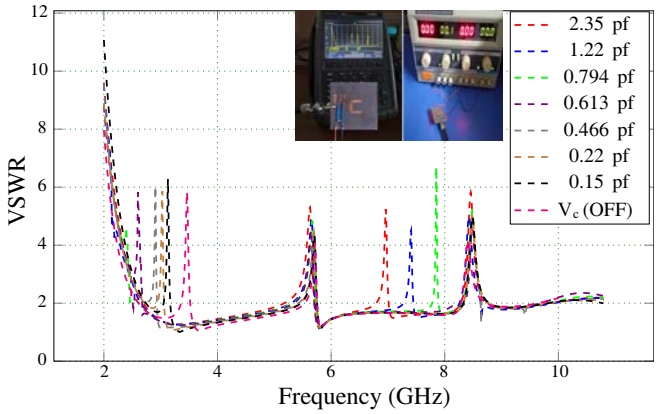

Figure 13. Experimental setup, Simulated VSWR of fork-type monopole antenna with TBMV-EBG and varactor diode.

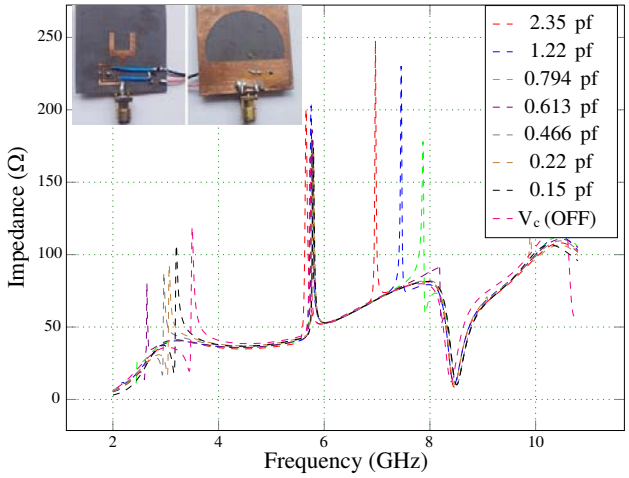

Figure 14. Fabricated prototype, simulated real part of impedance of fork type monopole antenna with TBMV-EBG and different varactor diode capacitances.

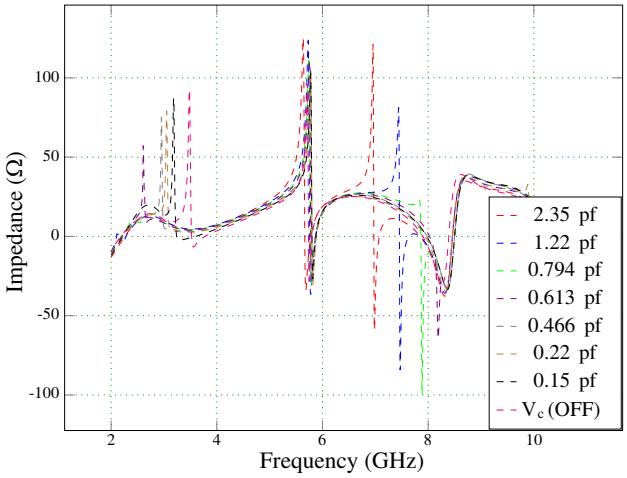

Figure 15. Simulated Imaginary part of impedance of fork type monopole antenna with TBMV-EBG and different varactor diode capacitances.

simulations using Ansys HFSS. Simulations are carried out by placing a varactor diode between the outer ring and middle ring of TBMV-EBG unit cell. The capacitance of varactor diode is varied from 2.35 pf to V_C(OFF) operated at reverse bias [33]. The simulated VSWRs for different capacitance values of varactor are shown in Fig. 13. It is observed that as the capacitance changes from 2.35 pf to V_C(OFF), the antenna shows tunable triple band-notched characteristics producing rejections at WIMAX, WLAN, and ITU bands respectively with different notching frequencies. Different modes of operations of the proposed triple band-notched antenna with simulated and measured results for specific varactor's capacitance and reverse bias voltage are shown in Table 3. Real and imaginary parts of impedances of the fork-type UWB antenna with TBMV-EBG for different values of capacitances are shown in Fig. 14 and Fig. 15, respectively. From Fig. 14, it is seen that for a particular value of varactor capacitance, the real part of band-notched antenna moves away from 50 Ω at the notching frequencies. Similarly for particular capacitance of varactor, imaginary part of impedance also goes away from 0 Ω where notching is present as shown in Fig. 15. The deviation of real and imaginary parts of impedance from 50 Ω and 0 Ω respectively are due to impedance mismatching at notched frequencies.

Simulated and measured VSWRs for 2.35 pf, 1.22 pf, 0.794 pf, 0.613 pf, and V_C(OFF) are depicted from Fig. 16 to Fig. 18(a), respectively. A strong agreement between simulated and experimental results

Table 3. Operating modes of proposed UWB antenna for different varactor capacitance (V_C).

Mode	Varactor Diode Capacitance V_C (pf)	Results Sim/Meas.	Notching Frequencies (GHz)
I	2.35 (0 V)	Simulated	5.62/6.90/8.45
		Measured	5.52/6.66/8.33
II	1.22 (2 V)	Simulated	5.65/7.46/8.45
		Measured	5.52/7.20/8.34
III	0.794 (4 V)	Simulated	5.67/7.84/8.50
		Measured	5.54/7.54/8.34
IV	0.613 (6 V)	Simulated	2.69/5.74/8.50
		Measured	3.10/5.52/8.34
V	0.466 (15 V)	Simulated	2.90/5.69/8.43
		Measured	2.96/5.52/8.33
VI	V_C(OFF)	Simulated	3.46/5.71/8.40
		Measured	3.39/5.70/8.47

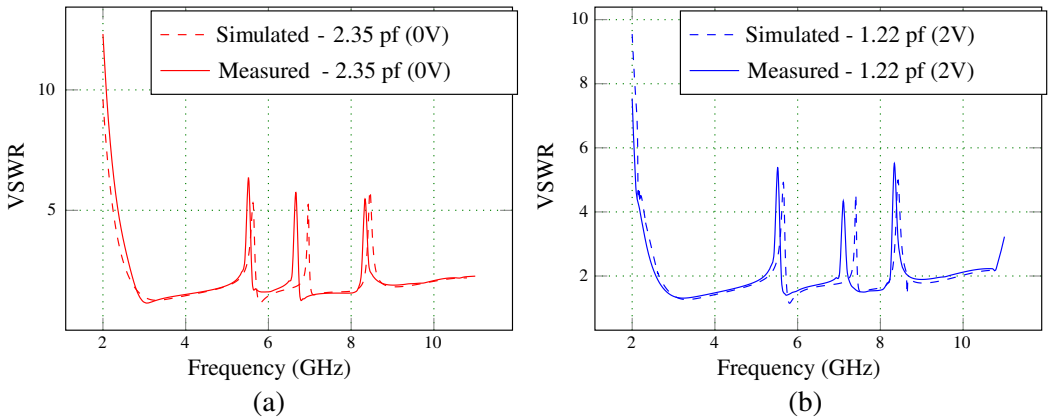

Figure 16. Simulated and measured VSWR at (a) 2.35 pf, and (b) 1.22 pf.

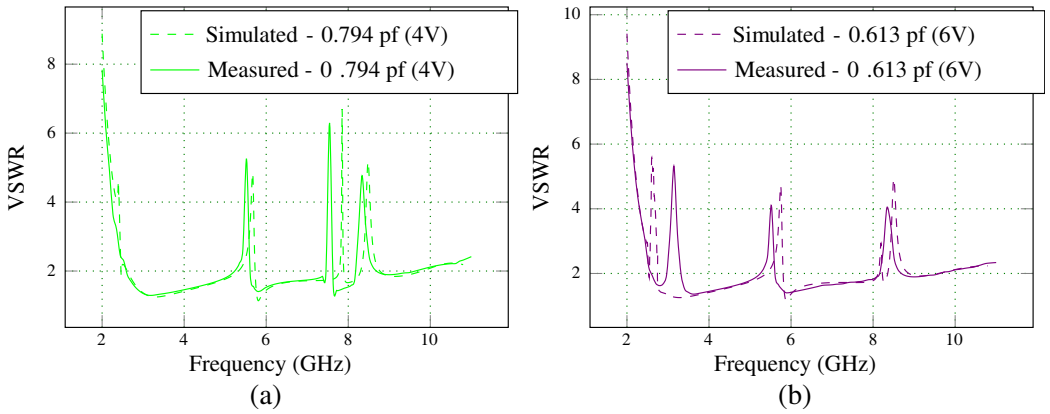

Figure 17. Simulated and measured VSWR at (a) 0.794 pf, and (b) 0.613 pf.

is obtained. Gain plots for different capacitances of varactor are shown in Fig. 18(b). Co-polarized and cross-polarized radiation patterns in H-plane and E-plane for fork-type UWB antenna with TBMV-EBG and varactor diode at 4.00 GHz and 8.00 GHz are shown in Fig. 19. The proposed antenna shows perfect bi-directional pattern in E-plane and omnidirectional pattern in H-plane at 4.00 GHz, but at higher frequencies due to the presence of higher order resonance modes, these patterns get slightly degraded.

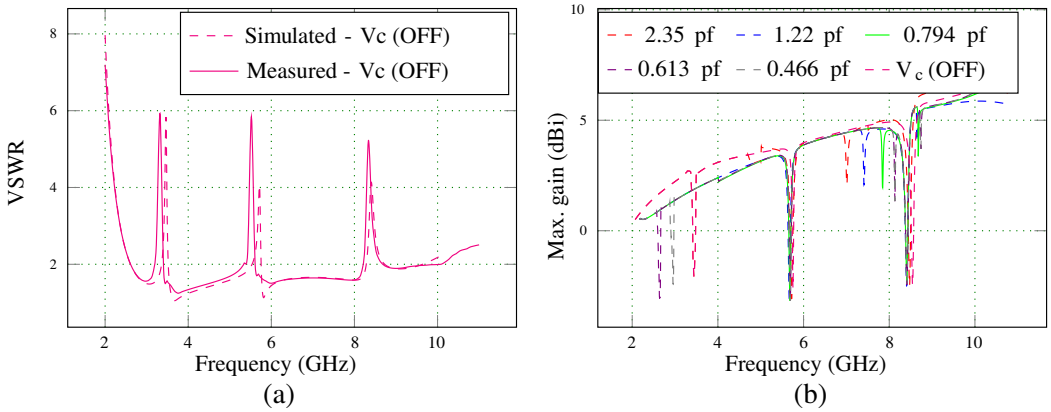

Figure 18. Simulated and measured VSWR at (a) V_C (OFF), and (b) antenna gain at different V_c.

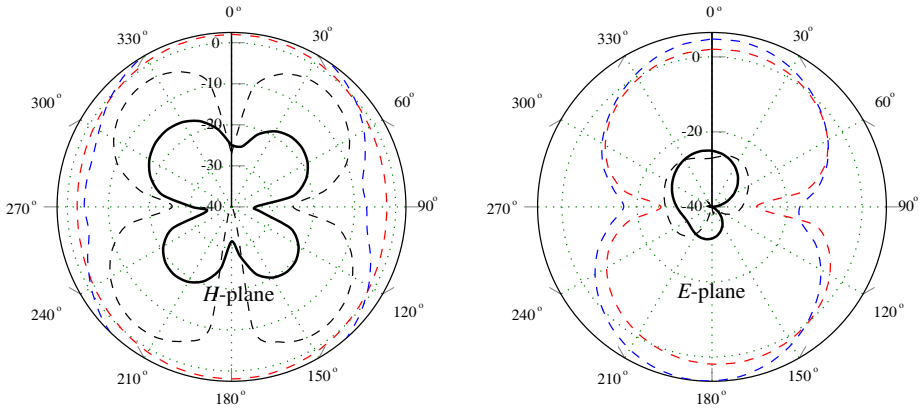

Figure 19. Radiation pattern for H-plane (y-z) and E-plane (x-z) of fork-type monopole antenna with TBMV-EBG and varactor diode (Co-pol 4.00 GHz, and 8.00 GHz), (X-pol 4.00 GHz, and 8.00 GHz).

5. CONCLUSION

An antenna with triple band-notch characteristics using a single TBMV-EBG cell is designed, simulated, and fabricated for ultra-wideband applications. Simulation results agree with measurement ones for rejections at 3.39 GHz, 5.78 GHz, and 8.60 GHz frequencies, respectively. Furthermore, tunable characteristics of the presented antenna with varactor diode are also simulated and experimentally verified. By changing the capacitance of varactor, the band-notched antenna is effectively tuned from 2.69 to 3.46, 5.71 to 7.84, and 8.40 to 8.50 GHz. The proposed UWB antenna exhibits triple band-notched characteristics using a single TBMV-EBG unit cell, triple-notch tuning using a single varactor diode with wide impedance bandwidth and good radiation characteristics. So, for ultra-wideband applications, in which multi-band rejections and multi-notch frequency tunability using a single antenna structure are desirable, the proposed antenna stands out to be a true candidate.

REFERENCES

1. Li, W., X. W. Shi, and Y. Q. Hei, "Novel planar UWB monopole antenna with triple band-notched characteristics," *IEEE Antennas Wireless Propag. Lett.*, Vol. 08, 1094–1098, Oct. 2009.
2. Nguyen, T. D., D. H. Lee, and H. C. Park, "Design and analysis of compact printed triple band-notched UWB antenna," *IEEE Antennas Wireless Propag. Lett.*, Vol. 10, 403–406, Apr. 2011.
3. Sarkar, D., K. V. Srivastava, and K. Saurav, "A compact microstrip-fed triple band-notched UWB monopole antenna," *IEEE Antennas Wireless Propag. Lett.*, Vol. 13, No. 01, 396–399, Mar. 2014.
4. Liu, W. and T. Jiang, "Design and analysis of a tri-band notch UWB monopole antenna," *2016 Progress in Electromagnetic Research Symposium (PIERS)*, 2039–2041, Shanghai, China, Aug. 8–11, 2016.
5. Rahman, M., D.-S. Ko, and J.-D. Park, "A compact multiple notched ultra-wide band antenna with an analysis of the CSRR-TO-CSRR coupling for portable UWB applications," *Sensors*, Vol. 17, No. 10, 2174, 2017.
6. Rahman, M. and J.-D. Park, "The smallest form factor UWB antenna with quintuple rejection bands for iot applications utilizing RSRR and RCSRR," *Sensors*, Vol. 18, No. 3, 911, 2018.
7. Mandal, T. and S. Das, "Design of dual notch band UWB printed monopole antenna using electromagnetic-bandgap structure," *Microwave and Optical Technology Letters*, Vol. 56, No. 9, 2195–2199, Sept. 2014.
8. Jaglan, N., B. K. Kanaujia, S. D. Gupta, and S. Srivastava, "Design and development of an efficient EBG structures based band notched UWB circular monopole antenna," *Wireless Personal Communication*, Vol. 96, No. 04, 5757–5783, Oct. 2017.
9. Yang, Y., Y. Yin, A. Sun, and S. Jing, "Design of a UWB wide-slot antenna with 5.2-/5.8-GHz dual notched bands using modified electromagnetic-bandgap structures," *Microwave and Optical Technology Letters*, Vol. 54, No. 4, 1069–1074, Apr. 2012.
10. Peng, L. and C. Ruan, "Design and time-domain analysis of compact multi-band-notched UWB antennas with EBG structures," *Progress In Electromagnetics Research B*, Vol. 47, 339–357, 2013.
11. Xu, F., Z. X. Wang, X. Chen, and X.-A. Wang, "Dual band-notched UWB antenna based on spiral electromagnetic-bandgap structure," *Progress In Electromagnetics Research B*, Vol. 39, 393–409, 2012.
12. Peng, L. and C. Ruan, "UWB band-notched monopole antenna design using electromagnetic-bandgap structures," *IEEE Trans. Microw. Theory Tech.*, Vol. 59, No. 4, 1074–1081, Apr. 2011.
13. Yazdi, M. and N. Komjani, "Design of a band-notched UWB monopole antenna by means of an EBG structure," *IEEE Antennas Wireless Propag. Lett.*, Vol. 10, 170–173, Feb. 2011.
14. Jaglan, N., S. D. Gupta, B. K. Kanaujia, and S. Srivastava, "Band notched UWB circular monopole antenna with inductance enhanced modified mushroom EBG structures," *Wireless Personal Communications*, Vol. 24, No. 2, 383–393, 2018.
15. Bhavarthe, P. P., S. S. Rathod, and K. T. V. Reddy, "Compact dual band gap electromagnetic bandgap structure," *IEEE Trans. Antennas Propag.*, Vol. 67, No. 1, 596–600, Jan. 2019.
16. Trimukhe, M. A. and B. G. Hogade, "Compact ultra-wideband antenna with triple band notch characteristics using EBG structures," *Progress In Electromagnetic Research C*, Vol. 93, 65–77, 2019.
17. Sievenpiper, D., L. Zhang, Romulo, J. Broas, N. Alexopolous, and E. Yablonovith, "High impedance electromagnetic surfaces with a forbidden frequency band," *IEEE Trans. Microw. Theory Tech.*, Vol. 47, No. 11, 2059–2074, Nov. 1999.
18. Yang, F. and Y. Rahmat-Samii, "Microstrip antennas integrated with electromagnetic band-gap (EBG) structures: A low mutual coupling design for array applications," *IEEE Trans. Antennas Propag.*, Vol. 51, No. 10, 2936–2946, Oct. 2003.
19. Li, T., H. Zhai, L. Li, C. Liang, and Y. Han, "Compact UWB antenna with tunable band-notched characteristic based on microstrip open-loop resonator," *IEEE Antennas Wireless Propag. Lett.*, Vol. 11, 1584–1587, Dec. 2012.

20. Wu, W., Y.-B. Li, R.-Y. Wu, C.-B. Shi, and T.-J. Cui, "Band-notched UWB antenna with switchable and tunable performance," *International Journal of Antennas and Propagation*, Vol. 2016, 1–6, Jun. 2016.
21. Tang, M.-C., H. Wang, T. Deng, and R. W. Ziolkowski, "Compact planar ultra-wideband antennas with continuously tunable, independent band-notched filters," *IEEE Trans. Antennas Propag.*, Vol. 64, No. 8, 3292–3301, May 2016.
22. Mohamed, H. A., A. S. Elkorany, S. A. Saad, and D. A. Saleeb, "New simple flower shaped reconfigurable band-notched UWB antenna using single varactor diode," *Progress In Electromagnetic Research C*, Vol. 76, 197–206, Aug. 2017.
23. Hua, C., Y. Lu, and T. Liu, "UWB heart-shaped planar monopole antenna with a reconfigurable notched band," *Progress In Electromagnetics Research Letters*, Vol. 65, 123–130, 2017.
24. Nejatijahromi, M., M. U. Rahman, and M. Naghshvarianjahromi, "Continuously tunable wimax band-notched UWB antenna with fixed WLAN notched band," *Progress In Electromagnetics Research Letters*, Vol. 75, 97–103, 2018.
25. Nejatijahromi, M., M. Naghshvarianjahromi, and M. Rahman, "Compact CPW fed switchable UWB antenna as an antenna filter at narrow-frequency bands," *Progress In Electromagnetics Research C*, Vol. 81, 199–209, 2018.
26. Hua, C. and Y. Lu, "Compact UWB bandpass filter with a reconfigurable notched band," *Int. J. RF Microwave Comput. Aided Eng.*, 1–7, Nov. 2017.
27. Shome, P. P., T. Khan, and R. H. Laskar, "CSRR-loaded UWB monopole antenna with electronically tunable triple band-notch characteristics for cognitive radio applications," *Microw. Opt. Technol Lett.*, 1–11, Dec. 2019.
28. Rahman, M., M. NagshvarianJahromi, S. S. Mirjavadi, and A. M. Hamouda, "Compact UWB band-notched antenna with integrated bluetooth for personal wireless communication and UWB applications," *Electronics*, Vol. 8, No. 2, 158, 2019.
29. Rahman, M., A. Haider, and M. Naghshvarianjahromi, "A systematic methodology for the time-domain ringing reduction in UWB band-notched antennas," *IEEE Antennas Wireless Propag. Lett.*, Vol. 19, 482–486, Mar. 2020.
30. Kingsly, S., D. Thangarasu, et al., "Tunable band-notched high selective UWB filtering monopole antenna," *IEEE Trans. Antennas Propag.*, Vol. 67, No. 8, 5658–5661, 2019.
31. Trimukhe, M. A. and B. G. Hogade, "Compact UWB antenna with tunable band-notch characteristics using varactor diode," *Progress In Electromagnetics Research C*, Vol. 97, 15–28, 2019.
32. Kapure, V., R. P. P. Bhavarthe, and S. S. Rathod, "A switchable triple-band notched UWB antenna using compact multi-via electromagnetic band gap structure," *Progress In Electromagnetics Research C*, Vol. 104, 201–214, 2020.
33. Skyworks, "SMV 123x series: Hyperabrupt function tuning varactors," *Datasheet*.